Some Modifications of the Free-Electron Model

Some Modifications of the Free-Electron Model

Takeshi NAKAJIMA

The Chemical Research Institute of Non-Aqueous Solutions

(Received December 9, 1952)

Synopsis

The perimeter-free-electron model which is rather the crude approximation for the calculation of the π-electronic spectra of a conjugated system is modified at some points. How the linear addition of a conjugated chain or phenyl groups to benzene will cause the red-shifts of their spectra with the increase of the length of chain or the number of phenyl is discussed by connecting them with each other so as to make the total one-electron wave function well behaved. The effects of the nuclear substitution with a heteroatom in the benzene ring are studied in the case of pyridine. The red-shifts of center of gravity of the actual singlets of pyridine, compared with that of benzene, is explained by the insertion of a suitable potential well along the perimeter-loop. As a typical non-alternant hydrocarbon, we take azulene and its absorption spectrum, electron density and red- or blue-shifts of the longest wave length transition on alkylation are calculated. These modifications raise the degree of approximation of the free-electron model up to that of the simple LCAO molecular orbital treatment.

I. Introduction

The idea of almost-free motion of the π-electrons in a planar conjugated molecule has always lain in the background of the molecular orbital treatment of these electrons.

To explain the spectra of conjugated polyenes Bayliss(1) adopted the idea of a Fermi gas of π-electrons in one dimension.

Using this idea, Simpson(2) recently discussed the spectra of porphine and its related compounds. Platt(3) extended and generalized this idea to the spectra of cata-condensed hydrocarbons. In these treatments the π-electrons travel in a one-dimensional loop of constant potential, so they are classified as "perimeter-free-electron model".

Previously Schmidt(4) adopted a large flat box containing π-electrons in benzene and its related compounds and named his method as "Kasten modell".

The introduction of the sinusoidal potentials or the corresponding potential wells into the "perimeter-free-electron model" was discussed by Bayliss(5) in the case of polyenes and by Simpson(6) and Kuhn(7) for the organic dyes and their related molecules.

(1) N. S. Bayliss, J. Chem. Phys., **16** (1948), 287.
(2) W. T. Simpson, J. Chem. Phys., **17** (1949), 1218.
(3) J. R. Platt, J. Chem. Phys., **17** (1949), 484.
(4) O. Schmidt, Zeits. f. phys. Chem., **B47** (1940), 1 and previous papers.
(5) N. S. Bayliss, J. Chem. Phys., **17** (1949), 1353.
(6) W. T. Simpson, J. Chem. Phys., **16** (1948), 1124.
(7) H. Khun, J. Chem. Phys., **17** (1949), 1198.

The effects of the cross-links on the perimeter-free-electron model was discussed by Oshika[8] with the linear polyacenes.

In this paper we discuss the effects of the length of the polyene chain attached to benzene, upon the absorption spectra (II), the red-shifts of the first excitation bands and the diminution of the mobility of π-electrons of polyphenyls with the increase of their molecular length (III), with pyridine, the shift of the center-of-gravity of actual singlets by nuclear substitution with a heteroatom in benzene (IV), and lastly for azulene, its absorption spectra, electron density and effects of some substitutions upon the spectra (V).

We shall see that these modifications raise the degree of approximation of the free-electron model up to that of the simple LCAO molecular orbital treatments.

II. The absorption spectra of styrene and its higher homologues

We consider the linear successive addition of two π-electrons to benzene as a linear polyene chain.

The molecular skeleton of the styrene type molecules, the length of the polyene chain of which is nl, is divided into two parts as shown in Fig. 1. $u_1(x_1)$ is the π-electron wave function of the benzene ring and $u_2(x_2)$ is that of polyene. The origin of the coordinate of each wave function is the point marked with letter u. Then $u_1(x_1)$ and $u_2(x_2)$ have the following forms respectively:

$$u_1(x_1)=a_1\cos\omega x_1+b_1\sin\omega x_1,$$
$$u_2(x_2)=\quad b_2\sin\omega x_2,$$

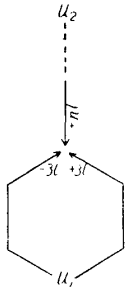

Fig. 1. The divided molecular skeleton of the styrene type molecule.

where the coordinate x is measured by one bond length l as a unit and ω is related to the orbital energy E by the following formula:

$$E=\frac{h^2\omega^2}{8\pi^2ml^2}$$

h=Planck's constant,
m=mass of electron.

The total one-electron wave functions Φ's are constructed by connecting $u_1(x_1)$ and $u_2(x_2)$. As Φ's must be one-valued and continuous at the point of connection, the following two conditions should be fulfilled:

equality: $\quad u_1(3)=u_1(-3)=u_2(n),$

continuity: $\quad \left(\frac{du_1}{dx_1}\right)_{x_1=3}-\left(\frac{du_1}{dx_1}\right)_{x_1=-3}+\left(\frac{du_2}{dx_2}\right)_{x_2=n}=0,$

that is,

$$a_1\cos 3\omega+b_1\sin 3\omega=a_1\cos 3\omega-b_1\sin 3\omega=b_2\sin n\omega,$$
$$2a_1\sin 3\omega-b_2\cos n\omega=0.$$

(8) Y. Oshika, Busseiron-Kenkyu, **29** (1950), 16 (Japanese).

These equations lead to the following secular equation:

$$\begin{vmatrix} -\sin n\omega & \cos 3\omega & \sin 3\omega \\ -\sin n\omega & \cos 3\omega & -\sin 3\omega \\ -\cos n\omega & 2\sin 3\omega & 0 \end{vmatrix} = 0.$$

Rewriting this, we have

$$\sin 3\omega = 0,$$
$$2\tan 3\omega = \cot n\omega.$$

The former is the symmetrical secular equation of benzene (reflection in a plane containing two origins and normal to the molecular plane). When n is 0, 2, 3 and 4, the solutions ω^2 of these equations are listed in Table 1 and arranged in Fig. 2. Six, eight, eight and ten π-electrons are filled in the two (the upper one is two fold degenerate), four, four and five molecular orbitals of the lowest energy respectively. The predicted center-of-gravity sequences and the observed sequences of singlets of styrene ($n=2$)[9] and 1-phenyl-pentadiene (1,3)[10] ($n=4$) are compared in Fig. 3. When $n=4$, on account of the lack of the observation of 1-phenyl-butadiene, we take 1-phenyl-pentadiene (1,3) and do not consider the difference caused by the methyl group. The prediction of the LCAO MO method are arranged for comparison. The bond length l is taken 1.39Å (of benzene) in all cases from want of the observed data. The extension of the length of the polyene chain causes the remarkable red-shift. The computed red-shift of the longest wave length transitions from the case $n=2$ to $n=4$ is 350 cm^{-1} which is smaller than the observed 550 cm^{-1}. This means that as the length of polyene chain becomes large π-electrons behave less freely. Moreover, the polarization of this transition changes as n increases from 2 to 4.

Table 1. Orbital energies ω^2 in styrene type molecules up to $\omega=\pi$.

$n=0$	$n=2$	$n=3$	$n=4$
			9.8696
		9.8696	8.7911
	9.8696	8.6224	5.9140
	8.3741	5.2882	4.3865
	4.6725	4.3865	4.1626
	4.3865	3.5706	2.4674
9.8696	2.4674	1.5685	1.2130
4.3865	1.0966	1.0966	1.0966
1.0966	0.9604	0.7090	0.5037
0.0000	0.0614	0.0421	0.0312

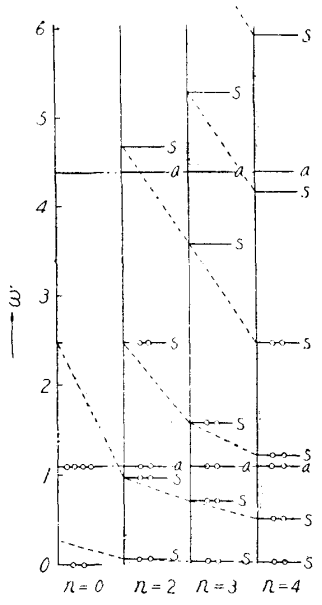

Fig. 2. Energy levels and shells of the styrene type molecules.

(9) J. R. Platt, J. Chem. Phys., **18** (1950), 1168.
(10) M. Pesterme and L. Wiligut, Monatsh. Chem., **66** (1935), 119.

For styrene, the calculation of the mobile order of bonds by Penny and Kynch[11] shows that l of the polyene chain is longer than that of the benzene ring. For this reason, and following the treatment of Bayliss, we extend the length of the polyene chain half the bond length and adopt the skeleton, n of which is 3, for styrene. The results are shown also in Fig. 3. The agreement of the calculated sequence with the observed one seems better than the case when $n=2$ but in this case the polarizations of bands are altered. The computed red-shift of the longest wave length transitions from the case $n=3$ to $n=4$ is 500 cm^{-1} and agrees well with the observed 550 cm^{-1}. But it is striking that the extension of the range of conjugation by half the bond length causes the blue-shift of the longest wave length transition.

For 1-phenyl-pentadiene (1,3) the extension of the length of the polyene chain causes the natural red-shift (the polarization being held) of the longest wave length transition and so the calculated transition for $n=5$ goes away further from the observed one compared with the case when $n=4$. In this case the extension by half the bond length is too large to be agreeable, as it is likely that the free motion of π-electrons in the polyene chain is impeded as compared with the case for styrene.

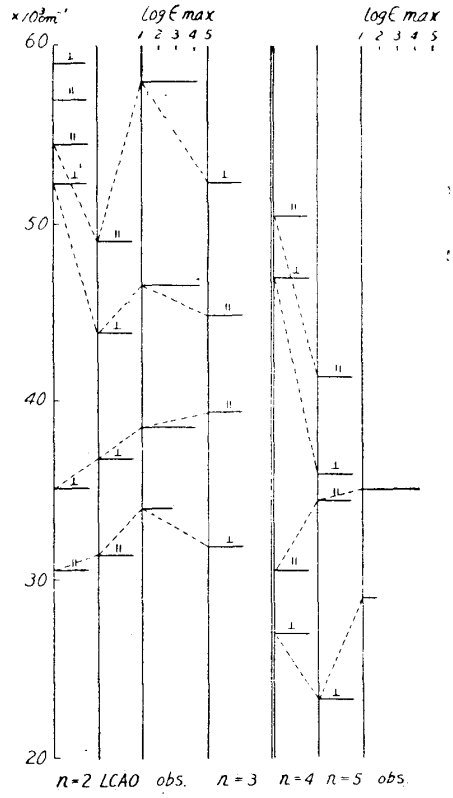

Fig. 3. Calculated centers of gravity and observed singlets excited states in styrene (left) and 1-phenyl-pentadiene(1.3)(right). (Vibrational structure omitted for simplicity. Length of horizontal lines in "observed" columns indicates intensity of transition from ground state according to scale at the top of the figure).

III. The successive addition of phenyls to benzene

Obviously, the linear successive additions of phenyl groups to benzene will cause the red-shift of the longest wave length transition, as the range of conjugation and the number of π-electrons concerned increase with the addition. The experimental results show that the larger the molecules become, the smaller the degree of the red-shift per phenyl becomes as in the case of polyene and diphenylene. In diphenyl, the length of the bond between the two benzene rings is longer (1.48Å) than that of any other bonds in the benzene rings (1.42Å).[12] As this seems to be the case with the larger homologues, it is not the good approximation to employ the free-electron model for these hydro-

(11) W. G. Penny and G. J. Kynch, Proc. Roy. Soc. (London), **A164** (1938), 409.
(12) J. Dahl, Indian J. Phys., **7** (1932), 43; C. A. **26** (1932), 4517.

carbons. The predicted transitions of the longest wave length by this method may be found at the longer wave length side of the actual ones because in these molecules π-electrons move not so freely as the application of the free-electron model is of good approximation. But the tendency of convergency of the displacements of the first absorption bands as the molecular length increases and some indications concerning the mobility of π-electrons will be obtained.

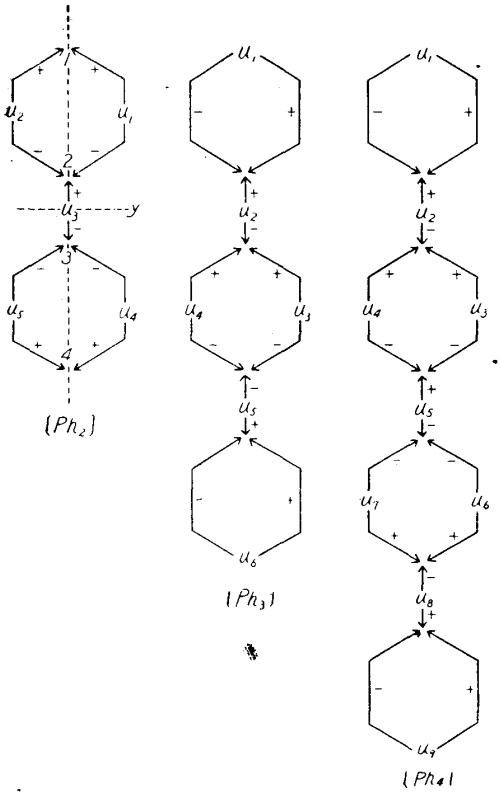

Fig. 4. The divided molecular skeletons of polyphenyls.

Now the molecular skeletons of diphenyl (Ph_2), *p*-terphenyl (Ph_3), *p*-quaterphenyl (Ph_4), *p*-quinoquiphenyl (Ph_5) and *p*-sexiphenyl (Ph_6) are divided into 5, 6, 9, 12 and 15 parts, each of which has its π-electron wave function u_1, u_2,$\cdots$as shown in Fig. 4. The total one-electron wave function Φ's is constructed by connecting u's so as to make Φ's the base of the irreducible representations of the symmetry group D_{2h}. For example, in diphenyl, the forms of u's which belong to each base are as follows:

B_{1u}:

$$u_1=u_2=u_4=u_5 = a_1\cos\omega x+b_1\sin\omega x,$$
$$u_3=a_3\cos\omega x,$$

B_{2g}:

$$u_1=u_2=-u_4=-u_5 = a_1\cos\omega x+b_1\sin\omega x,$$
$$u_3=b_3\sin\omega x,$$

B_{3g}:

$$u_1=-u_2=u_4=-u_5 = a_1\cos\omega x+b_1\sin\omega x,$$
$$u_3=0,$$

A_u:

$$u_1=-u_2=-u_4=u_5 = a_1\cos\omega x+b_1\sin\omega x,$$
$$u_3=0.$$

The conditions of equality and continuity at the four connection points are given as follows:

B_{1u}:

at the points 1 and 4

eq. : self-evident,

conti.: $2a_1\sin\frac{3}{2}\omega-2b_1\cos\frac{3}{2}\omega=0,$

at the points 2 and 3

eq. : $a_1\cos\frac{3}{2}\omega-b_1\sin\frac{3}{2}\omega=a_3\cos\frac{\omega}{2},$

conti.: $2a_1\sin\frac{3}{2}\omega+2b_1\cos\frac{3}{2}\omega+a_3\sin\frac{\omega}{2}=0,$

B_{2g}:

at the points 1 and 4

eq. :
conti.: } same as B_{1u},

at the points 2 and 3

eq. : $a_1\cos\frac{3}{2}\omega - b_1\sin\frac{3}{2}\omega = b_3\sin\frac{3}{2}\omega,$

conti.: $2a_1\sin\frac{3}{2}\omega + 2b_1\cos\frac{3}{2}\omega - b_3\cos\frac{\omega}{2} = 0,$

B_{3g} and A_u:

at the points 1 and 4

eq. : $a_1\cos\frac{3}{2}\omega + b_1\sin\frac{3}{2}\omega = 0,$

conti.: self-evident,

at the points 2 and 3

eq. : $a_1\cos\frac{3}{2}\omega - b_1\sin\frac{3}{2}\omega = 0,$

conti.: self-evident.

For the higher homologues we can write these conditions without difficulty. These equations easily lead to the following recursion formula of the secular determinants for each base. When n (the number of benzene ring) is odd

$$|\mathrm{Ph}_n|_{B_{1u}} = = |D| \times |\mathrm{Ph}_{n-1}|_{B_{1u}} - |B| \times |\mathrm{Ph}_{n-1}|_{B_{2g}},$$
$$|\mathrm{Ph}_n|_{B_{2g}} = |C| \times |\mathrm{Ph}_{n-1}|_{B_{1u}} + |A| \times |\mathrm{Ph}_{n-1}|_{B_{2g}},$$
$$|\mathrm{Ph}_n|_{B_{3g}} = \cos^{\frac{n+1}{2}}\left(\frac{3\omega}{2}\right)\sin^{\frac{n-1}{2}}\left(\frac{3\omega}{2}\right),$$
$$|\mathrm{Ph}_n|_{A_u} = \cos^{\frac{n-1}{2}}\left(\frac{3\omega}{2}\right)\sin^{\frac{n+1}{2}}\left(\frac{3\omega}{2}\right),$$

and when n is even

$$|\mathrm{Ph}_n|_{B_{1u}} = |A| \times |\mathrm{Ph}_{n-1}|_{B_{1u}} - |B| \times |\mathrm{Ph}_{n-1}|_{B_{2g}},$$
$$|\mathrm{Ph}_n|_{B_{2g}} = |C| \times |\mathrm{Ph}_{n-1}|_{B_{1u}} - |D| \times |\mathrm{Ph}_{n-1}|_{B_{2g}},$$
$$|\mathrm{Ph}_n|_{B_{3g}} = |\mathrm{Ph}_n|_{A_u} = \cos^{\frac{n}{2}}\left(\frac{3\omega}{2}\right)\sin^{\frac{n}{2}}\left(\frac{3\omega}{2}\right),$$

where

$$|A| = \begin{vmatrix} 2\cos\frac{3}{2}\omega & \sin\frac{\omega}{2} \\ \sin\frac{3}{2}\omega & \cos\frac{\omega}{2} \end{vmatrix}, \quad |B| = \begin{vmatrix} \cos\frac{3}{2}\omega & -\cos\frac{\omega}{2} \\ 2\sin\frac{3}{2}\omega & \sin\frac{\omega}{2} \end{vmatrix}, \quad |C| = \begin{vmatrix} 2\cos\frac{3}{2}\omega & -\cos\frac{\omega}{2} \\ \sin\frac{3}{2}\omega & \sin\frac{\omega}{2} \end{vmatrix},$$

$$|D| = \begin{vmatrix} \cos\frac{3}{2}\omega & \sin\frac{\omega}{2} \\ 2\sin\frac{3}{2}\omega & \cos\frac{\omega}{2} \end{vmatrix}, \quad |\mathrm{Ph}_1|_{B_{1u}} = 2\sin\frac{3}{2}\omega, \quad |\mathrm{Ph}_1|_{B_{2g}} = -2\cos\frac{3}{2}\omega.$$

The last two ($n=1$) are the secular determinants of benzene. Choosing the two variables x and y as

$$x = \sin\frac{\omega}{2}, \qquad y = \cos\frac{\omega}{2},$$

the determinants for B_{1u} and B_{2g} become when n is even

$$|Ph_n|_{B_{1u}}=(12x^4-13x^2+2)|Ph_{n-1}|_{B_{1u}}+xy(12x^2-7)|Ph_{n-1}|_{B_{2g}},$$
$$|Ph_n|_{B_{2g}}=(12y^4-13y^2+2)|Ph_{n-1}|_{B_{2g}}+xy(12y^2-7)|Ph_{n-1}|_{B_{1u}},$$

and when n is odd

$$|Ph_n|_{B_{1u}}=(12x^4-11x^2+1)|Ph_{n-1}|_{B_{1u}}+xy(12x^2-7)|Ph_{n-1}|_{B_{2g}},$$
$$|Ph_n|_{B_{2g}}=(12y^4-11y^2+1)|Ph_{n-1}|_{B_{2g}}+xy(12y^2-7)|Ph_{n-1}|_{B_{1u}},$$

where

$$|Ph_1|_{B_{1u}}=2x(3-4x^2), \qquad |Ph_1|_{B_{2g}}=2y(3-4y^2).$$

Accordingly, we get the following simple relation between the determinants of B_{1u} and B_{2g} regardless of the value of n

$$|Ph_n(x)|_{B_{1u}}=|Ph_n(y)|_{B_{2g}}$$

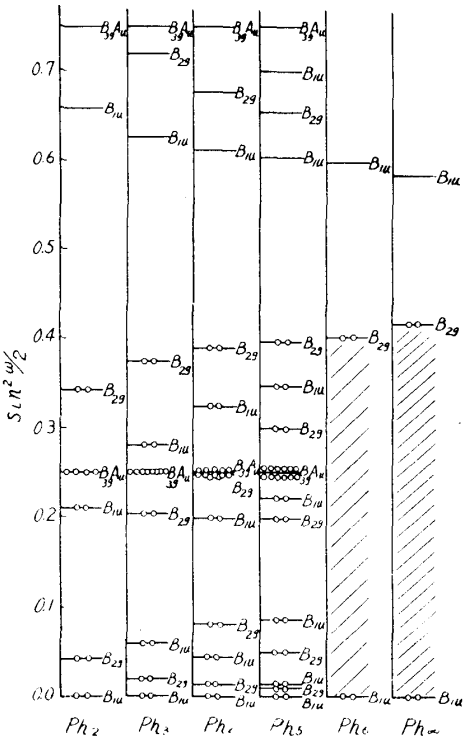

Fig. 5. Energy levels and shells of polyphenyls.

and so by solving only the secular equation for B_{1u} about x we can obtain the energy y for B_{2g} directly. The secular equations for B_{3g} and A_u are handled easily. In Fig. 5 up to the case when $n=5$, thus obtained energy levels $x^2=\sin^2\frac{\omega}{2}$ are arranged and 12(Ph_2), 18(Ph_3), 24(Ph_4) and 30(Ph_5) π-electrons are filled in the 6 (B_{3g} and A_u are mutually degenerate), 9 (twofold degenerated B_{3g} and A_u are mutually degenerate), 12 (twofold deg. B_{3g} and likewise deg. A_u are mutually degenerate) and 15 (threefold deg. B_{3g} and twofold deg. A_u are degenerate mutually) molecular orbitals of the lowest energy respectively. The higher unfilled levels are omitted in the figure as these levels are symmetric with the value $\sin^2\frac{\omega}{2}=0.5$ and their names are obtained only by interchanging B_{1u} for B_{2g} and *vice versa*. All the longest wave length transitions are $B_{2g}\rightarrow B_{1u}$ and polarized parallel to the longer axis of the molecules. The calculated and observed longest

Table 2. Comparison of calculated center-of-gravity with observed singlets in polyphenyls.

Molecule	Calculated trans. energy.		Observed singlets. cm^{-1}	Discrepancy between calc. and obs. singlets. cm^{-1}	Red shift calculated. cm^{-1}	Red shift observed. cm^{-1}
	$\Delta\omega^2$	cm^{-1}				
Ph_2	2.020	32,100	39,200	7,100	6,500	7,100
Ph_3	1.607	25,600	35,100	9,500	3,000	2,400
Ph_4	1.420	22,600	32,700	10,100	1,700	1,000
Ph_5	1.313	20,900	31,700	10,800	1,100	800
Ph_6	1.246	19,800	30,900	11,100		
Ph_∞	1.052	16,700	29,000 (?)	12,000(?)		

wave length transitions are tabulated in Table 2.[13] The prediction of the limiting case when $n\to\infty$ is added also in the table and Fig. 5. This can be calculated easily as follows: when n approaches infinity we can equate nearly as $|\mathrm{Ph}_{n-1}|_{B_{2g}}\simeq|\mathrm{Ph}_n|_{B_{2g}}=0$ and $|\mathrm{Ph}_{n-1}|_{B_{1u}}\simeq|\mathrm{Ph}_n|_{B_{1u}}=0$, so that we get the highest filled energy level for B_{2g} by equating $|C|=0$ and the lowest unfilled level for B_{1u} by $|B|=0$. The π-electrons of infinite numbers are filled in the continuous region between the two lowest solutions of the Eq. $|C|=0$, namely, from the level $\sin^2\frac{\omega}{2}=0$ up to the level $\sin^2\frac{\omega}{2}=\frac{5}{12}$. An imaginary molecule, Ph_∞ would be a typical insulator.

As has been inferred, the predicted transitions are in the longer wave length side of the observed ones in all cases. But the predictions of the red-shifts of the first excitation bands with the increase of the molecular lengh is rather good, though the calculated convergency is slower than that of the observation. The convergency of the observed transitions and the calculated ones are shown in Fig. 6. As n approaches infinity the observed transition seems to converge nearly on 29,000 cm^{-1}. The slower convergency of the calculation is related with the divergency of the discrepancy between the calculated and observed transitions for each molecule as the molecule becomes large. This increase of the discrepancy is seen in column 5 in Table 2. The dicrepancy of the case when $n\to\infty$ attains nearly 12,000 cm^{-1}. They mean that the limiting structures in which the bonds connecting the benzene rings are double bonds and the electrons or charges separate at the both ends of molecules contribute less to the normal state and so the π-electrons can cross over these bonds less freely as the molecular length increases. The absolute discrepancy in diphenyl may be attributed to the non-coplanarity of diphenyl in liquid phase.[14]

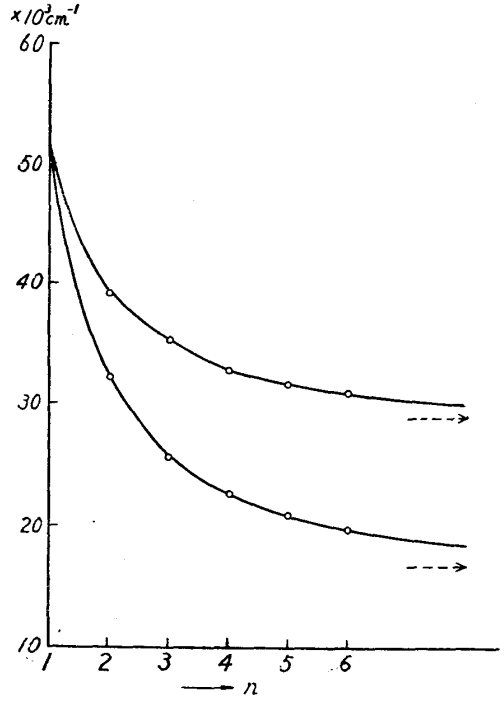

Fig. 6. Calculated(lower) and observed (upper) red-shifts of the longest wave length transitions of polyphenyls.

IV. The bathochromic shift of pyridine

The bathochromic shift of the center-of-gravity of the actual singlets of pyridine, compared with that of benzene, was calculated in the LCAO MO

(13) A. E. Gillam and D. H. Hey, J. Chem. Soc., (1939), 1170.
(14) H. Suzuki, Symposium on Electronic States, 6 (1951), 1 (Japanese).

approximation by Nordheim and Sponer.[15] In the following customary assumptions concerning the Coulomb integral H_{kk}, exchange integral H_{mk} and overlap integral Δ_{mk}

$$H_{kk}=\alpha+\delta_k\beta$$

$$H_{mk}=\begin{cases}\beta & \text{if } \varphi_m \text{ and } \varphi_k \text{ belong to adjacent atoms}\\ 0 & \text{otherwise for } m\neq k\end{cases}$$

$$\Delta_{kk}=1 \qquad \Delta_{mk}=0 \text{ for } m\neq k$$

where $\alpha=$ the Coulomb integral in benzene and $\beta=$ exchange integral, they assumed $\delta_N=2$, and δ_c (of C atoms nearest to the N atom)$=\frac{\delta_N}{8}$ for pyridine. These assumptions give 6.12 eV for the predicted average height of the actual levels in good agreement with the value 6.14 eV from the observations.

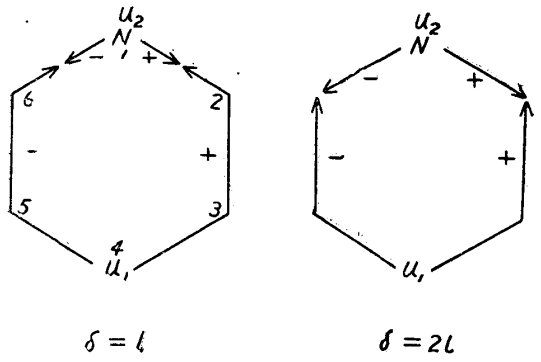

Fig. 7. The divided molecular skeleton of pyridine.

Corresponding to this alternation of the Coulomb integral of the N atom, here we introduce the suitable potential well at the position of the N atom along the perimeter of pyridine. The molecular skeleton is divided into two parts u_1 and u_2 as in Fig. 7. $u_2(x_2)$, the wave function of the potential well, extends over one bond length or two. $u_1(x_1)$ and u_2 (x_2) have the following form respectively:

$$u_1(x_1)=a\cos\omega x_1+b\sin\omega x_1, \qquad \omega^2=\frac{8\pi^2ml^2E}{h^2},$$

$$u_2(x_2)=a'\cos\omega' x_2+b'\sin\omega' x_2, \qquad \omega'^2=\frac{8\pi^2ml^2(E+V)}{h^2}.$$

where V is the depth of the potential well.

When the length of the potential well is one bond length, the secular equations, obtained from the equality and continuity at the points of connection, become

$$\text{sym.} \qquad \tan\frac{5}{2}\omega=-\frac{\omega'}{\omega}\tan\frac{\omega'}{2},$$

$$\text{antisym.} \qquad \tan\frac{5}{2}\omega=-\frac{\omega}{\omega'}\tan\frac{\omega'}{2},$$

where sym. and antisym. are symmetric to a plane through the two origins and normal to the molecular plane and antisymmetric to the same plane respectively.

By putting

$$\omega'^2=\omega^2+\lambda^2, \qquad \lambda^2=\frac{8\pi^2ml^2V}{h^2},$$

these equations can be solved by the graphical method. This time, $h^2/8\pi^2ml^2$ is assigned 15,500 cm^{-1} from the average height of the benzene singlets, 6.28 eV.

(15) G. P. Nordheim and H. Sponer, J. Chem. Phys., **20** (1952), 285.

When $\lambda^2=1$ and $\lambda^2=2$, ($V=15{,}500\,cm^{-1}$ and $31{,}000\,cm^{-1}$ respectively) the calculated energy levels are arranged in Fig. 8, where the lowest level is omitted in all cases. The levels of benzene are added for comparison. The bathochromic shift of the center-of-gravity of singlets of pyridine, compared with that of benzene, is $160\,cm^{-1}$ and $540\,cm^{-1}$ respectively. The observed shift is $1135\,cm^{-1}$ (0.14 eV). By assigning a larger value to the parameter V, we may make the computed shift agree well with the observed one. But comparing the electronegativity of N atom with that of C atom, it is not plausible to assign such a large depth to the potential well for N atom.

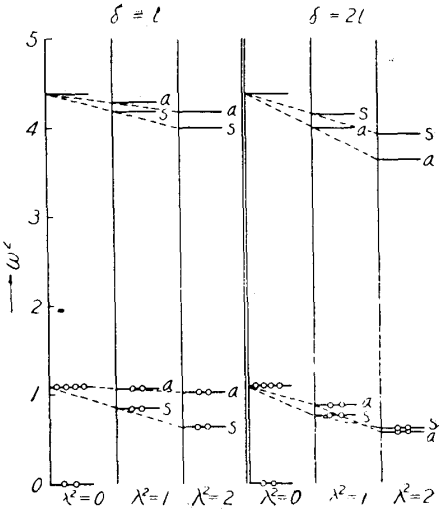

Fig. 8. Energy levels and shells of benzene and pyridine.

When the length of the potential well covers two bond length, the secular equations become

$$\text{sym.} \qquad \tan 2\omega = -\frac{\omega'}{\omega}\tan\omega',$$

$$\text{antisym.} \quad \tan 2\omega = -\frac{\omega}{\omega'}\tan\omega'.$$

The predicted levels are shown also in Fig. 8. The corresponding red-shift of the center-of-gravity of pyridine is $660\,cm^{-1}$ ($\lambda^2=1$) and $1670\,cm^{-1}$ ($\lambda^2=2$). The good agreement with the observed shift would lie between $\lambda^2=1$ and $\lambda^2=2$ ($V=15{,}500\,cm^{-1}$ $31{,}000\,cm^{-1}$).

As seen in the figure, when the potential well covers one bond length, the increase of the depth of the potential well causes the more remarkable red-shifts to the sym. levels than to the antisym. ones, but when the potential well covers two bonds length the red-shifts of the antisym. levels are more enhanced than that of sym. ones. The extension of the length of the potential well to two bonds length corresponds to the small alternation of the Coulomb integrals of the two carbon atoms, nearest to the N atom in the LCAO approximation. It is notable that in the simple LCAO MO approximation neglecting overlapping if we do not change these Coulomb integrals, the antisym. levels remain unaltered and the red-shifts of sym. levels are the same for the lowest unfilled and the highest filled levels of benzene so there is no red-shift of the center-of-gravity of singlets, thus obtained, however large value we may assign to the Coulomb integral of N atom. But in our treatment the insertion of the potential well of a finite length always causes the red-shift of the center-of-gravity.

In computing the effects of a heteroatom, there is another way of the free-electron model, that is the perturbation method. We take the normalized wave functions of benzene as the zeroth order normalized wave functions for pyridine. Then the energy levels of pyridine are given as

$$E_n + V\int_{-\delta/2l}^{\delta/2l} \Phi_n^2(x)dx,$$

E_n: energy level of benzene,
V : depth of the potential well,
δ : length of the potential well along the perimeter,

by the first order perturbation theory. Thus the two fold degeneracies of the highest filled and lowest unfilled energy levels of benzene are removed and the first and second excitation bands of pyridine show the red-shift compared with the center-of-gravity of singlets of benzene. But the center-of-gravity of these four singlets of pyridine remains the same as for benzene, no matter in what extent we may change the parameter V and δ. The same circumstance occurs in the simple LCAO MO perturbation method.

V. Non-alternant hydrocarbon

We take azulene as a typical non-alternant hydrocarbon. The perimeter-free-electron model can not explain the differences of the characteristic behaviors of π-electrons between azulene and naphthalene. The effects of the cross-linkage must be taken into consideration because it must play an important role. The study on azulene was carried out by several authors in the LCAO MO[16), (17), (18), (19)] approximation.

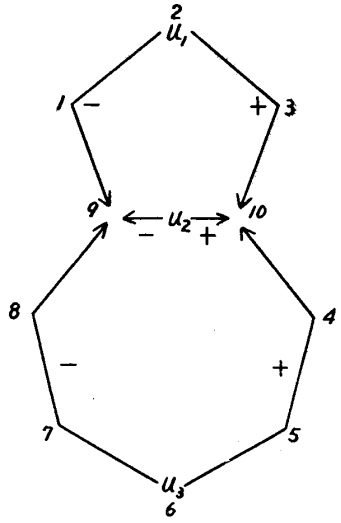

Fig. 9. The divided molecular skeleton of azulene.

The molecular skeleton of azulene is divided into three parts $u_1(x_1)$, $u_2(x_2)$ and $u_3(x_3)$ as shown in Fig. 9. The plane of symmetry includes the line joining three origins of these parts and is normal to the molecular plane. The wave functions symmetric to this plane are

$$u_1(x_1) = a_1\cos\omega x_1,$$
$$u_2(x_2) = a_2\cos\omega x_2,$$
$$u_3(x_3) = a_3\cos\omega x_3.$$

When we connect these wave functions so that they may be continuous and one valued as before, the following secular equations are obtained approximately: (when the bond angle deviates from $2\pi/3$, the condition of continuity at a point of connection does not hold in a strict sense but for a small deviation we can use it approximately.)

$$\tan\frac{\omega}{2} = -(\tan 2\omega + \tan 3\omega).$$

The anti-symmetrical wave functions are

$$u_1(x_1) = b_1\sin\omega x_1,$$
$$u_2(x_2) = b_2\sin\omega x_2,$$
$$u_3(x_3) = b_3\sin\omega x_3,$$

(16) B. Pullman, M. Mayot and G. Berthier, J. Chem. Phys., **18** (1950), 257.
(17) E. Clar, J. Chem. Soc., (1950), 1823.
(18) D. E. Mann, J. R. Platt and H. B. Klevens, J. Chem. Phys., **17** (1949), 481.
(19) R. D. Brown, Trans. Faraday Soc., XLIV (1948), 984.

and the corresponding secular equations are

$$\tan\frac{\omega}{2} = -\frac{\tan 2\omega \tan 3\omega}{\tan 2\omega + \tan 3\omega}.$$

Table 3. Normalized wave functions of azulene.

Sym.	$u_1(x_1)$	$u_2(x_2)$	$u_3(x_3)$
sym.	0.3015	0.3015	0.3015
sym.	$0.4188\cos 0.622x_1$	$0.1412\cos 0.622x_2$	$-0.4619\cos 0.622x_3$
antisym.	$0.2371\sin 0.885x_1$	$0.5428\sin 0.885x_2$	$0.4970\sin 0.885x_3$
sym.	$0.4996\cos 1.169x_1$	$-0.4158\cos 1.169x_2$	$0.3713\cos 1.169x_3$
antisym.	$0.5584\sin 1.334x_1$	$0.3931\sin 1.334x_2$	$-0.3148\sin 1.334x_3$
sym.	$0.2859\cos 1.758x_1$	$-0.4172\cos 1.758x_2$	$-0.4997\cos 1.758x_3$

Table 4. Comparison of calculated center-of-gravity with observed singlets in azulene.

Trans. type.	Pol.	Calculated trans. energy. $\Delta\omega^2$	Calculated trans. energy. cm^{-1}	Observed singlets. cm^{-1}
^1L_b	⊥	1.311	19,400	14,400
^1L_a	∥	1.724	25,500	27,500
^1B_b	∥	1.941	28,700	34,000
^1B_a	⊥	2.354	34,800	48,000
^1C_b	∥	2.938	43,500	41,000

The coefficients a_1, a_2, a_3 and b_1, b_2, b_3 can be calculated by making the resultant total one-electron wave function normalize to unity. The obtained complete wave functions are tabulated in Table 3. The calculated energy levels are compared with those through the perimeter-free-electron model in Fig. 10. The predicted sequence of singlets is tabulated in Table 4, and arranged also in Fig. 10 including the results of the LCAO MO method and the observed sequence. This time, the calculation is carried out by standardizing the color of benzene, 205 $m\mu^{-1}$. Names used by Platt and Coulson are added. The prediction agrees well with the observation to the same extent as in the LCAO MO approximation.

We can also calculate the electron density. The electron densities of the points of *C* atom are shown in Fig. 11. But these do not normalize and agree so well with the electron density of LCAO MO method. When we integrate over the one bond length from the middle point of a bond up to that of the

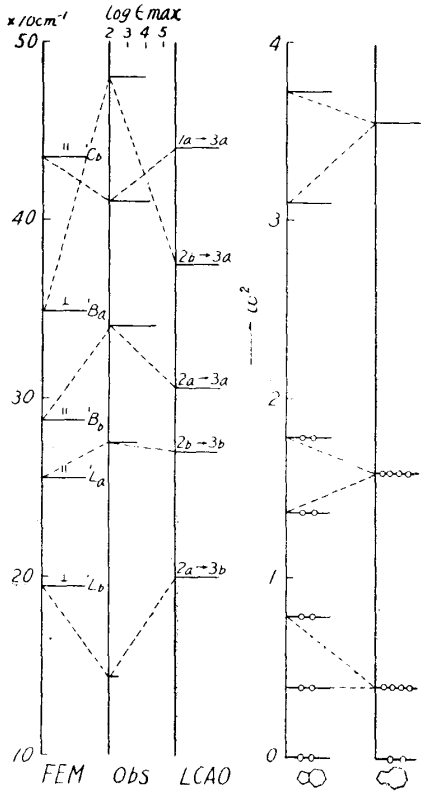

Fig. 10. Calculated centers of gravity and observed singlet excited states of azulene (left, see note under Fig. 3) and its energy levels and shells (right).

adjacent bonds (there are two these bonds on the position 9 and 10), the integrated normalized electron densities agree well with the electron densities of the LCAO MO as shown also in Fig. 11. It is remarkable that the two calculations, started from the two completely different standpoints agree so well. In addition, we can calculate the electron density on a bond by integrating over the one bond length. The results are shown in Fig. 11. The physical meaning of these quantity is not known but they seem as a crude measure of the bond length as the bond orders of the LCAO MO though the complete agreement between these quantities and actual bond length are not secured.

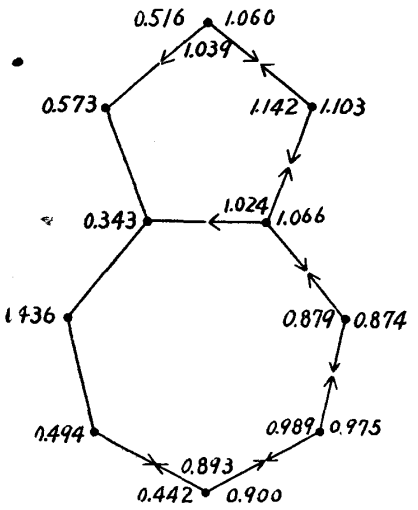

left : point charges by FEM.
right inner : electron densities by LCAO.
right outer : integrated densities by FEM.

Fig. 11. Electron densities of azulene.

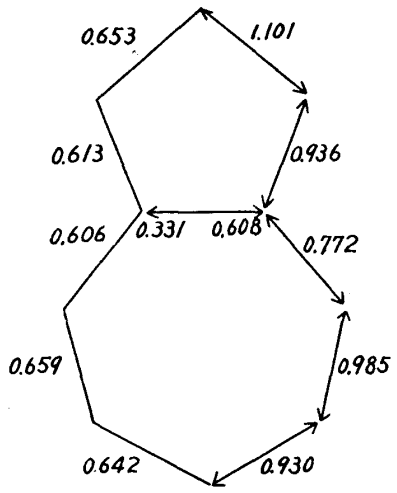

Fig. 12. Integrated density distribution of electrons on bonds by FEM (right) and mobile order of bonds by LCAO (left)

The batho- or hypsochromic shift of the first excitation band of azulene on alkyl substitution was discussed by Pullman and others in the LCAO MO approximation.[16] The observed shift is as follows:

position of methylation, degree of shift,

3 and 5 batho. $1>5$,

2,4 and 6 hypso. $2>6>4$.

Obviously, the shift of the first excitation band on methylation is caused by the hyper-conjugation and the inductive effect of methyl group. Inclusion of the hyper-conjugation in calculation is rather complicated so we consider the positive inductive effect of the methyl group only by inserting the potential barrier along the perimeter of azulene at the position where the methyl group is attached. For example, for 2-methylazulene the shift is calculated by the first order perturbation method as follows

$$V(0.2859^2\int_{-\delta/2l}^{\delta/2l}\cos^2 1.758x_1dx_1-0.5584^2\int_{-\delta/2l}^{\delta/2l}\sin^2 1.334x_1dx_1)=0.022V>0.$$

V: height of a potential barrier,

δ : length of a potential barrier.

For other methylated azulenes, the calculated shifts are

3-methyl	$-0.238V<0$,
4-methyl	$0.148V>0$,
5-methyl	$-0.022V<0$,
6-methyl	$0.181V>0$,

where we assume $\delta/l=1$. The degree of shift is as follows:

batho.	$1>5$,
hypso.	$6>4>2$.

Although we do not take into account the hyper-conjugation and consider only the inductive effect of methyl group, the calculated shifts of the longest wave length transitions agree with the observation qualititatively. The calculated order of the shifts agrees with that of observation, except that 2-methylation causes the smallest hypsochromic shift (observed one is largest). The same circumstance occurs in the LCAO MO treatment which takes into account the hyper-conjugation explicitly.

Conclusive remarks

We modified the perimeter-free-electron model which promises poor results when applied to the several examples, here treated, especially in considering the effects of cross-links and heteroatoms. The predictions, obtained by thus refined free-electron orbital method, are agreeable with the observation to the same extent as by the simple LCAO MO approximation in spite of the completely different starting models between them.

The RFEM (the refined free electron model) is a kind of the LCMO (the linear combination of molecular orbitals) as seen in the several examples in the preceding chapters. The simple LCAO MO approximation, restricted to combine atomic *p*-orbitals, predicts only a finite number of one-electron states. The RFEM, however, leads to an infinite number of states. The additional free-electron states are due to the implicit consideration of atomic orbitals of energy higher than the *p*-orbitals such as *d*- and *f*- orbitals. The overlap integral between adjacent atoms is often neglected in the simple LCAO approximation. The inclusion of overlap causes little difference but its neglect is rather unreasonable. In the RFEM, however, the corresponding overlap is always considered tacitly. For hydrocarbons, the usefulness of the FEM exists in that a parameter, introduced in it, is only a bond length. But in a strict sense, it is not an experimental bond length, but, so to speak, an effective bond length. The effective bond length can not be derivable formally from the experimental one but it seems obvious that the larger the latter becomes, the smaller the former becomes. The relation between these two bond lengths is like that between the exchange integral β and the actual bond length through the overlap integral in the LCAO MO approximation.

The present author wishes to thank Prof. H. Tominaga and Assist. Prof. H. Azumi, Faculty of Science, for their guidances and to Mr. H. Kon for his helpful discussions.